Dynamic Light Scattering Studies of Polystyrene in Tetrahydrofuran at Intermediate Scattering Vectors

Mamta Bhatt and Alex M. Jamieson*

Department of Macromolecular Science, Case Western Reserve University, Cleveland, Ohio 44106. *Received January 29, 1988; Revised Manuscript Received April 12, 1988*

ABSTRACT: Static and dynamic light scattering characteristics of narrow molecular weight distribution polystyrenes (M_w = 0.09–20 × 10^6) in a good solvent, tetrahydrofuran, have been investigated for the first time, over the small to intermediate qR_g region by homodyne photon correlation spectroscopy. The z-average radius of gyration, $\langle R_g^2\rangle_z^{1/2}$; the second virial coefficient, A_2; the infinite dilution translational diffusion coefficient, $\langle D_t\rangle_z^0$; and the dimensionless decay rate $\Gamma^* = \Gamma_e(q,c)/(q^3kT/\eta_0)$, where Γ_e is the first cumulant of the decay function, have been extracted self-consistently by using cumulant, double-exponential, and multiexponential methods of analyses. The values, $\Gamma^*(q)$, characteristic of a single coil have been obtained by extrapolating Γ_e to c = 0. These have been compared with experimental results for the ratio $\rho = R_g/\langle R_h^{-1}\rangle^{-1}$. We find that $\Gamma^*(q)$ for polystyrene chains is surprisingly well represented by a theoretical prediction of Akcasu and Gurol for a nondraining Gaussian chain model with nonpreaveraged Oseen hydrodynamic interactions. Likewise, values of ρ are consistent with a theoretical prediction for a nondraining Gaussian coil with internal friction. Existing theories of $\Gamma^*(q)$ and ρ for self-avoiding chains are not in agreement with our experimental results.

Introduction

In recent years, major advances have been made in understanding the static and dynamic behavior of flexible swollen chains in dilute solution.[1] New theoretical techniques have provided clearer insights into the molecular origin of thermodynamic and transport properties; e.g., numerical simulations using Monte Carlo methods on self-avoiding walks[2-4] and analytical approaches based on the renormalization group approach[5-8] have led to improved modeling of polymer chain statistics. Likewise, efforts have been made to improve the original hydrodynamic theory of Kirkwood and Riseman[9] and incorporate the effects of excluded volume,[10,11,68] internal friction,[65] and draining[7,8] into the dynamical modeling of polymer chains in dilute solution.

Many previous experiments have focused on polystyrene (PS) chains of narrow molecular weight distribution in good and Θ solvents and these data have been compared with theoretical models of linear flexible chains. Static light scattering experiments have been reported for polystyrene in benzene (BZ),[12-14] toluene (TOL),[15,16] ethylbenzene (ETBZ),[17] and tetrahydrofuran (THF).[17,28,29] The similar radii of gyration and second virial coefficients observed in all these solvent systems suggest similar solvating powers for polystyrene. Also, dynamic measurements in benzene,[13] toluene,[15] and ethylbenzene[17] have reported comparable hydrodynamic radii, R_h, resulting in comparable ratios of the static to dynamic radii, $\rho = R_g/\langle R_h^{-1}\rangle^{-1} \cong 1.57$, in these systems. This compares with values of $\rho \cong 1.27$ for polystyrenes in Θ solvents.[41,42] On the other hand, the hydrodynamic radii measured for PS in the good solvent THF[17,18,21-23] are reported to be 15% larger than those reported in the aromatic solvents, and hence $\rho \cong 1.3$ for this system. This result is of considerable interest since ratios of static to dynamic radii are predicted[6,64] to exhibit universal behavior for polymer–solvent systems in the crossover from the Θ to the good solvent asymptote provided the strength of the hydrodynamic interaction is constant. Thus the value $\rho \cong 1.5$, for PS in aromatic good solvents is in agreement with theoretical predictions in the nondraining self-avoiding chain limit by Oono and Kohmoto,[6] while the value $\rho \cong 1.27$ for PS in Θ solvents is consistent with a Monte Carlo calculation by Zimm[24] for a nondraining Gaussian coil. The result $\rho \cong 1.3$ for PS in the good solvent THF clearly conflicts with the concept of universality,[6,64] and we may likewise note that experimental studies by Noda et al.[43-45] for poly(α-methylstyrene) in good and Θ solvents yielded $\rho \cong 1.5$, independent of solvent quality. It is pertinent to note, however, that two recent theoretical treatments[7,8] conclude that the values of ρ should be constant, independent of solvent quality, provided the hydrodynamic interaction remains independent of chain expansion. Thus Douglas and Freed have interpreted changes in the ρ value between Θ and good solvents in terms of an increase in solvent draining on chain expansion, while Tsunashima et al.[37] have likewise suggested the variation in ρ may be due to a decrease in the strength of internal friction[65] with chain expansion.

It is of further interest to extend dynamic light scattering analyses to large scattering vectors ($qR_g \gg 1.0$) where the effective decay rate, Γ_e, of the photon correlation function is influenced by internal (configurational) motions of the polystyrene chains. It is, in fact, possible to separate the contributions of internal and external motions to the relaxation spectrum. Such analyses, however, require multiexponential fits or Laplace transforms of the photon correlation function and involve difficult questions regarding the uniqueness of the obtained fits. Thus, we confine ourselves in this paper to reporting information on the effective decay rate Γ_e or, more precisely, on the quantity $\Gamma^*(q) = \lim_{c=0} \Gamma_e(q)\eta_0/kTq^3$. Theory predicts that $\Gamma^*(q)$ should again exhibit universal scaling properties for flexible polymer chains at a specified intensity of the excluded-volume interaction and for comparable hydrodynamic interaction characteristics. Experimentally, when plotted versus qR_g, $\Gamma^*(q)$ decreases monotonically toward a constant asymptotic value, corresponding to $\Gamma_e \propto q^3$ for polystyrenes in both Θ[46,54]- and good[36,37,54,69]- solvent systems. This is consistent with anticipated behavior for nondraining flexible polymer coils.[67]

For polystyrene chains, different asymptotic values of $\Gamma^*(q)$ have been obtained for good and Θ solvents in the large qR_g region. These values are, however, in disagreement with most theoretical predictions. Studies on the Θ solvents cyclohexane[46] and *trans*-decalin[54] have reported $\Gamma^* \cong 0.045$, which is 15–20% smaller than the asymptote predicted by the Akcasu–Gurol[56] theory for Gaussian chains. It is also in disagreement with the theoretical value ($\Gamma^* = 0.027$) obtained by Oono[74] for nondraining Gaussian chains with nonpreaveraged Oseen hydrodynamics. In a recent report[73] on another Θ system, polyisoprene in 1,4-dioxane, a value of $\Gamma^* \cong 0.48$ has been obtained. For polystyrene in the good solvent, benzene, Nemoto et al.[36] have reported an asymptotic value of ≅0.055 in the large

0024-9297/88/2221-3015$01.50/0

qR_g region. This value is 22–25% smaller than the theoretical estimates of Benmouna and Akcasu for nondraining self-avoiding chains and appears closer to the value obtained by Oono ($\Gamma^* = 0.05$) for highly swollen chains using a nonpreaveraged Oseen tensor. More recently, Tsunashima et al.[37] have reported measurements of Γ^* in high molecular weight polyisoprenes (PIP) of narrow molecular weight distribution in cyclohexane (CH), a good solvent, and deduced an asymptotic value $\Gamma^* \cong 0.06$, larger than that observed for polystyrene. The latter value is, surprisingly, in agreement with the Akcasu–Gurol[56] prediction for nondraining Gaussian chains using nonpreaveraged hydrodynamic interactions. Tsunashima et al.[37] postulate that the source of deviations between prediction and experiment for polystyrenes lies in its comparative conformational rigidity. Further, it was also suggested[37] that a rationale for the apparent applicability of the Gaussian coil model to chains in good solvents may be sought by evaluating the hydrodynamic interactions within the Domb–Gillis–Wilmers[66] configurational distribution function for self-avoiding chains and invoking a contribution from internal friction.[65] It is, hence, clearly of interest to generate additional data on the dynamic light scattering properties of polymer chains in the intermediate qR_g region.

We have investigated the static and dynamic light scattering properties of dilute solutions of narrow distribution polystyrenes in THF at 25 °C in the range $0.03 < qR_g < 6$. The experimental quantities of interest are the radius of gyration, R_g; the second virial coefficient, A_2; the infinite dilution translational diffusion coefficient, D_t^0; and the effective decay rate Γ_e. We have previously reported extensive measurements of D_t^0 for PS in THF[17,21] which was determined to contain trace amounts (0.09%) of water. This study begins by investigating these parameters, using scrupulously dry[25] THF and then extends to include new measurements of the photon correlation function over a wide range of values of $qR_g > 1.0$. Values of the effective decay rate Γ_e extrapolated to infinite dilution at $qR_g > 1.0$ are reported here for PS in THF for the first time. These quantities are used to test molecular theories on the dynamics of a single polymer chain in a good solvent.

Experimental Section

Materials. Narrow-distribution PS standards were obtained from the Pressure Chemical Co. (Pittsburgh) and were used without further purification. The weight-average molecular weights ranged from 0.09×10^6 to 20×10^6. All samples were characterized by methods of static light scattering in our laboratory and in each case the molecular weights were reproduced to within a few percent of their specified values as shown in Table I. Tetrahydrofuran was obtained from Aldrich Chemical Co. as ACS spectrograde THF. Due to its hygroscopic[25] nature, it was further purified by refluxing with $LiAlH_4$ for 12 h and then distilled in a dry inert N_2 atmosphere immediately before use. Using this method of solvent preparation, we obtained "dry" THF which was also free of dust or other inhomogeneities. This was confirmed by monitoring fluctuations in the scattered intensity from pure solvent, which were found to be less than 1% for THF clarified in the above manner.

Physical Properties. The refractive index of the solvent was measured at 25 °C in an Abbe Refractometer (Series 361-XU) and was determined to be $n_{25°C} = 1.407$. The specific refractive index increment, dn/dc, of PS in THF was determined by using a Brice Phoenix differential refractometer at 6328 Å and was obtained to be $dn/dc = 0.192$ cm^3/g at 25 °C. The viscosity of the solvent was measured at different temperatures by using a Cannon Ubbelohde viscometer which was calibrated by other solvents, viz., toluene, methanol, and ethylbenzene. The flow times were selected to ensure that kinetic energy corrections are negligible. The viscosity of THF at 25 °C was determined to be 0.465 cP. The specific gravity of the solvent at this temperature was 0.88. The specific gravity and viscosity were also measured at several elevated temperatures. The η_0 values obtained for THF at 30, 40, and 52 °C were 0.457, 0.404, and 0.362 cP, respectively.

Table I
Static Light Scattering Characteristics of Polystyrene in Tetrahydrofuran at 25 °C

polymer	$10^{-6}M_w$[a]	M_w/M_n	$10^{-6}M_w$[b]	$\langle R_g^2\rangle^{1/2} \pm 5\%$, Å	$10^3A_2 \pm 7\%$, mol cm^3 g^{-2}
AD-6	0.09	1.06	0.094		0.591
AD-7	0.3	1.06	0.32		0.410
AD-8	0.6	1.10	0.63		0.369
AD-9	0.9	1.10	0.92	400	0.309
AD-10	1.8	1.10	1.82	580	0.256
AD-11	3.84	1.04	3.77	915	0.219
AD-12	5.48	1.15	5.47	1180	0.201
AD-13	8.42	1.17	8.32	1356	0.183
AD-14[c]	20.0	1.20	22.0	2435	0.141

[a] Suppliers specifications. [b] Experimentally measured values. [c] Fujita plot.

Sample Preparation. Dilute solutions of PS in THF were made by weighing individual samples in a Perkin-Elmer microbalance, Model AD-2, with an accuracy of ±0.01 mg. The purified dry solvent was directly transferred into dust-free volumetric flasks containing preweighed PS samples. All solutions (except $M_w = 20 \times 10^6$) were shaken for several hours to promote complete dissolution. For light scattering measurements the samples were sealed in dust-free scattering cells and centrifuged at 5000 rpm for 30 min prior to performing the experiments. This procedure was followed for all samples except $M_w \simeq 2 \times 10^7$, where high-speed centrifugation could separate out the high molecular weight fractions of the polymer to the bottom of the cell. The solutions containing samples for $M_w = 20 \times 10^6$ were equilibrated at room temperature for at least 24 h and then shaken intermittently over a period of 72 h before being transferred to the dust-free scattering cells. The scattered intensity from stock solutions was monitored for several days and reproducible measurements indicated complete dissolution. All solutions were checked for optical clarity by monitoring the scattered intensity for 80–100 runs of 1-s duration each and only those solutions were used where the fluctuations in the scattered intensity were less than ±2%. This ascertained the absence of dust particles or other nonhomogeneities which are sources of parasitic scattering and prevent a meaningful interpretation of the time correlation function. Further, all static light scattering measurements were repeated after several days and found to be within 2% of each other.

Methods. All scattering experiments were performed on a Brookhaven Instrument Corp. spectrometer comprising a BI 2000 goniometer and a BI2030 AT correlator with a SpectraPhysics 15-mW He/Ne laser ($\lambda = 6328$ Å). Cylindrical sample cells were used and mounted at the center of a temperature-controlled, refractive index matched bath. Temperatures were controlled at 25 ± 0.1 °C for all experiments. Absolute calibration of the spectrometer was made with benzene (Spectro-grade, Aldrich Chemicals) for which the absolute Rayleigh ratio at $\lambda = 6328$ Å was $R_{V,V+H}(90) = 11.84 \times 10^{-6}$ as reported by Pike et al.[32] All measurements were made at 20–120° scattering angles. For dynamic measurements the intensity autocorrelation function was measured on a 264-channel BI2020 correlator with a multiple sampling time option. In addition, eight delay channels were used to determine the measured base line for a given autocorrelation function. To probe relaxation processes occurring on widely differing time scales, multiple sampling times were used to obtain the correlation function. For this, the 264 real time channels in the correlator were split into four successive groups of 64 channels each and the eight delay channels were added to the last group. The sample time for each group could then be selected as a power of 2 times the base sample time, τ_1, employed for the first group. Hence, the first group consists of 64 equally spaced sample times, τ_1, and the successive groups could have a sample time, $\tau_{i+1} = \tau_i \times 2^n$ where $i = 1, 2, 3, 4$ and $n = 0, 1, 2, 3, ..., 8$. This multiple sampling time option allowed us to obtain information about different parts of the relaxation spectrum simultaneously, resulting in an accurate determination of the form of the line-width distribution function, $G(\Gamma)$. Only those intensity–intensity time

correlation functions, $C(\tau)$, where the difference between the calculated and measured base lines was less than 0.1% were used for data analysis. Dynamic measurements were repeated at least twice to check for reproducibility and were found to be within 2–4% of each other. The data was further analyzed on an IBM/AT computer and a VAX 11/780.

Static Measurements. The excess Rayleigh ratio due to concentration fluctuations is obtained from the absolute excess scattered intensity and for vertically polarized incident light can be expressed as

$$\frac{Kc}{R(\theta)} = \frac{1}{M_w P(\theta)} + 2A_2c + 3A_3c^2 + ... \quad (1)$$

where $K = 4\pi^2 n_0^2 (dn/dc)^2 / N_A \lambda^4$ and A_2 & A_3 are the second and third osmotic virial coefficients, respectively. n_0 is the refractive index of the solvent, N_A is Avogadro's number, c is the concentration in g/mL, and θ is the scattering angle. $P(\theta)$, the particle scattering function, can be expressed as

$$P^{-1}(\theta) = \left[1 + \frac{16\pi^2 n_0^2 \langle R_g^2 \rangle \sin^2(\theta/2)}{3\lambda^2} + ... \right] \quad (2)$$

Equation 1 in the limit of zero angle and infinite dilution yields

$$\lim_{\substack{c \to 0 \\ \theta \to 0}} \frac{Kc}{\Delta R(\theta)} = \frac{1}{M_w} \quad (3)$$

For low molecular weights ($\leq 0.6 \times 10^6$) measurements were made at one angle ($\theta = 40°$) and the molecular weights were extracted from eq 3, where $P(\theta) = 1$. At high molecular weights ($M_w > 0.6 \times 10^6$) the measurements were performed over a range of concentrations and scattering angles. The Zimm[26] plots exhibited noticeable curvature due to a finite third virial coefficient and hence square-root plots[27] were used to determine the molecular weights. Thus a plot of $(Kc/\Delta R(\theta))_{\theta \to 0}^{1/2}$ versus c was used to determine A_2, and $\langle R_g^2 \rangle_z$ was obtained from the slope of $(Kc/\Delta R(\theta))_{c \to 0}^{1/2}$ versus $\sin^2(\theta/2)$. For $M_w = 20 \times 10^6$ it was necessary to generate a Fujita[16] plot to obtain an accurate estimate of the molecular weight.

Dynamic Measurements. Dynamic measurements were performed on the polymer samples AD-11, AD-12, AD-13, and AD-14. The quantities determined were the average line width, Γ_e; the z-average translational diffusion coefficient, $\langle D_t^0 \rangle_z$; and the corresponding Stokes radius, R_h. For samples AD-11 and AD-12, $qR_g \lesssim 1.0$ in the angular range studied and the average line width, Γ_e, can be determined by cumulant[19] analysis of the correlation function. Here, we define the normalized distribution function $G(\Gamma)$ of relaxation time constants $\Gamma = D_t q^2$

$$\int G(\Gamma)\, d\Gamma = 1 \quad (4)$$

and hence the average line width Γ_e and the variance μ_2/Γ_e^2

$$\Gamma_e = \int_0^\infty G(\Gamma)\Gamma\, d\Gamma \quad (5)$$

$$\mu_2 = \int_0^\infty (\Gamma - \Gamma_e)^2 G(\Gamma)\, d\Gamma \quad (6)$$

Then, the measured intensity–intensity correlation function $G^2(\tau)$ can be related to $G(\Gamma)$ by

$$G^2(\tau) = A(1 + b|g^1(\tau)|^2) \quad (7)$$

$$|g^1(\tau)| = \int_0^\infty G(\Gamma) \exp(-\tau\Gamma)\, d\Gamma \quad (8)$$

where A is the background (or the base line), b is a constant which is a function of the detecting optics and accounts for the nonideal point detector, and $|g^1(\tau)|$ is the normalized electric field autocorrelation function. $|g^1(\tau)|$ can be expanded in a Taylor series

$$|g^1(\tau)| = \exp[(-\Gamma_e\tau)\{1 + (\Gamma - \Gamma_e)^2\tau^2/2! + ...\}] \quad (9)$$

and a polynomial expansion of $\ln |g^1(\tau)|$ leads to

$$\ln |g^1(\tau)| = -\Gamma_e\tau + \frac{\mu_2(\Gamma_e\tau)^2}{\Gamma_e^2(2!)} - ... \quad (10)$$

where the zeroth order moment Γ_e can be related to the z-average translational diffusion coefficient $\langle D_t \rangle_z$ by

$$\Gamma_e = \langle D_t \rangle_z q^2 \quad (11)$$

where $q = (4\pi n_0 \sin\theta/2)/\lambda$.

For the higher molecular weight polymer samples, AD-13 and AD-14, the experimental parameters extend into the intermediate qR_g region, $qR_g > 1$, where the second-order cumulant fit proves inadequate. This occurs because the correlation function becomes increasingly nonexponential due to contributions from intramolecular motions and multimodal line-width distributions are obtained. Therefore, higher order cumulant fits or other methods of analysis must be used to obtain $G(\Gamma)$, the line-width distribution function. In principle, $G(\Gamma)$ can be computed by Laplace inversion of $g^1(\tau)$ in eq 8. However, in practice, the correlation function contains noise and then Laplace inversion becomes a very difficult ill-conditioned problem. Thus, several approximation procedures[33-36,46-54,70,71] have been developed and used to obtain the form of $G(\Gamma)$.

For our experiments in the intermediate qR_g region, two approaches in particular are useful, viz., the double-exponential (DEXP) and the multiexponential (MEXP) fitting techniques. The former method approximates the $G(\Gamma)$ distribution as a weighted sum of two Dirac δ functions

$$G(\Gamma) = a_1\delta(\Gamma - \Gamma_1) + a_2\delta(\Gamma - \Gamma_2) \quad (12)$$

which corresponds to

$$|g^1(\tau)| = [a_1 \exp(-\Gamma_1\tau) + a_2 \exp(-\Gamma_2\tau)] \quad (13)$$

where a_1 and a_2 are the amplitudes of the scattered intensity corresponding to the characteristic line widths Γ_1 and Γ_2. Therefore, $a_1 + a_2 = 1$ and $\Gamma_e = a_1\Gamma_1 + a_2\Gamma_2$.

The multiexponential sampling technique approximates $G(\Gamma)$ by a set of logarithmically spaced discrete single exponentials

$$G(\Gamma) = \sum_j P_j \delta(\Gamma - \Gamma_j) \quad (14)$$

where P_j are the weighting factors of the δ function and

$$\sum_j P_j = 1 \quad \text{(normalization condition)}$$

$$\Gamma_j/\Gamma_{j-1} = K \quad (K = \text{constant})$$

Substituting for $G(\Gamma)$ in eq 8 yields

$$|g^1(\tau)| = \sum_j P_j \exp(-\Gamma_j\tau) \quad (15)$$

where each of the P_j contributions is linearly independent. Following the procedure of Ostrowsky et al.[33,34] the correlation function is sampled at a series of exponentially spaced sample times, i.e., τ, $\exp(\pi/\omega_{max})\tau$, $\exp(2\pi/\omega_{max})\tau$, ... Then it has been shown[33] that the Nyquist sampling theorem can be applied along with an interpolation procedure[34] to fully reconstruct the correlation function at all values of τ limited only by the band limit ω_{max}. The experimental noise in the $G^2(\tau)$ data defines ω_{max}, which is a relative measure of the resolution of the obtained fit; i.e., $G(\Gamma)$ cannot be resolved at points closer than π/ω_{max}. Hence, the higher the value of ω_{max} the better the resolution in $G(\Gamma)$. Then a linear least-squares procedure is used where

$$\sum_{i=1}^{M} (G^2(\tau) - \sum_{n=1}^{N} a_n \exp(-\Gamma_i\tau))^2 \quad (16)$$

is minimized and a semilog plot of a_n versus Γ is obtained. The values of the average line width, Γ_e, obtained from the above analysis were compared to results obtained from the third- and fourth-order cumulant and double-exponential fits. It was found that all Γ_e values were within 2–4% of each other at the smaller angles, but at the higher angles the agreement was only within 5–7%. The multiexponential analysis consistently gave better fits to the experimental data $G^2(\tau)$, as assessed from plots of the residuals

$$\frac{G^2(\tau) - G^2(\tau)_c}{G^2(\tau)} \quad (17)$$

where $G^2(\tau)_c$ is the obtained fit. Figure 1A gives an example of

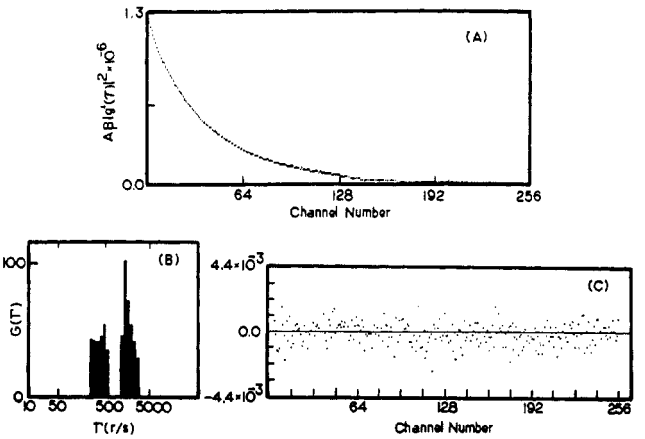

Figure 1. (A) Example of a normalized correlation function for the solution of the highest molecular weight sample (AD-14) in THF with $c = 0.09 \times 10^{-5}$ g cm^{-3} at $\theta = 50°$ and $\tau_1 = \tau_2 = 35$ μs, $\tau_3 = 70$ μs, $\tau_4 = 140$ μs. (B) The corresponding distribution for $G(\Gamma)$ versus Γ. (C) Plot of the residuals versus channel number.

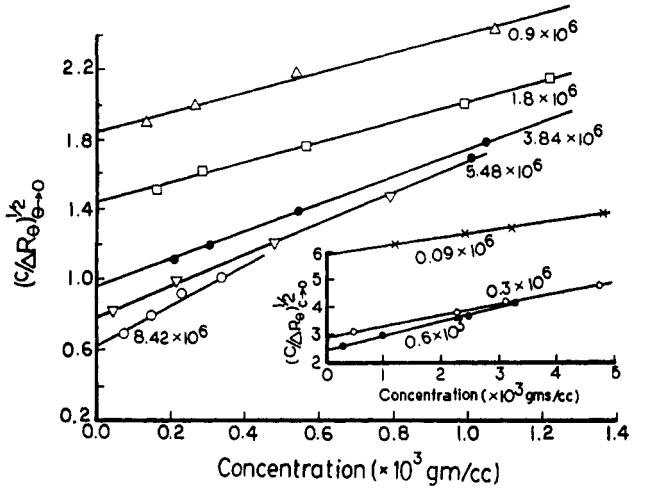

Figure 2. Berry plot of PS in THF for molecular weights from 0.09×10^6 to 8.42×10^6. $(c/\Delta R_\theta)^{1/2}$ as a function of concentration extrapolated to zero angle.

a normalized autocorrelation function obtained for a solution of the highest molecular weight sample (AD-14) in THF with $c = 0.0609 \times 10^{-3}$ g/cm^3 at a scattering angle of $\theta = 50°$. Figure 1B,C shows the result of a multiexponential fit on this data together with a plot of the corresponding residuals.

Results

Static Properties. Berry plots of PS in THF (for $M_w < 20 \times 10^6$), i.e., $(c/\Delta R\theta)_{c=0}^{1/2}$ versus c and $(c/\Delta R\theta)_{\theta=0}^{1/2}$ versus $\sin^2 \theta/2$, are shown in Figures 2 and 3. The results of the static measurements are listed in Table I. The molecular weights we determined are in good agreement with the suppliers specifications. The radii of gyration appear to be systematically about 5% smaller than values reported earlier[17] from our laboratory and are comparable to those reported in other good solvents.[12-17,28,29] Likewise, the second virial coefficients, A_2, obtained in this study are approximately 10–15% smaller than those reported previously[17] but are still larger than those typically obtained in the aromatic good solvents, viz., benzene, ethylbenzene, and toluene. In the molecular weight range investigated in this study, log–log plots of $\langle R_g^2 \rangle_z^{1/2}$ and A_2 versus M_w are linear and can be described by the following least-squares fits

$$\langle R_g^2 \rangle_z^{1/2} = (0.1589 \pm 0.01) M_w^{0.57 \pm 0.01} (A) \quad (18)$$

$$A_2 = (0.0125 \pm 0.007) M_w^{-0.266 \pm 0.003} \text{ (cm}^3 \text{ mol)/g}^2 \quad (19)$$

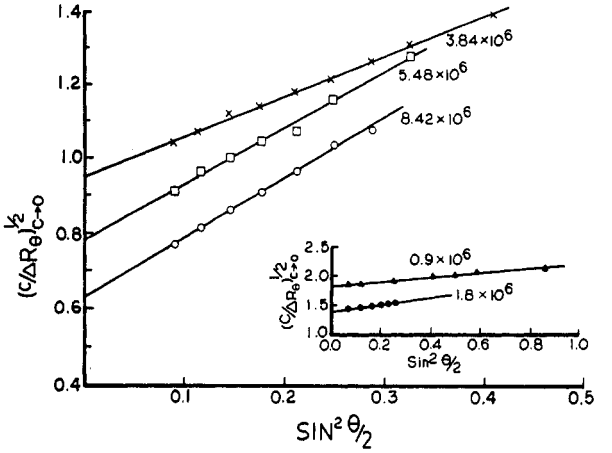

Figure 3. Berry plot of PS in THF for $M_w = 0.9 \times 10^6$ to 8.42×10^6. $(c/\Delta R_\theta)^{1/2}$ as a function of scattering angle extrapolated to zero concentration.

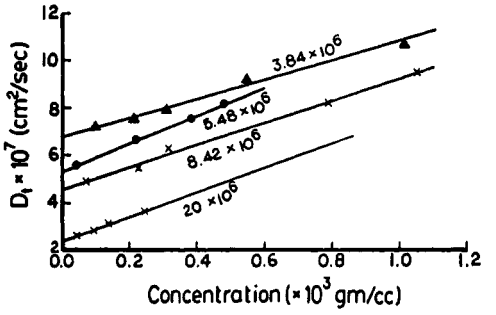

Figure 4. Concentration dependence of the translational diffusion coefficients for samples AD-11, AD-12, AD-13, and AD-14.

Table II
Static Light Scattering Characteristics of Polystyrene in Tetrahydrofuran at 25 °C

sample	$10^8 D_t^0$, cm^2/s	R_h, Å	$10^{-2} k_d$, cm^3/g	$\rho = R_g/R_h$
AD-11	6.82	695	5.71	1.32
AD-12	5.31	893	11.14	1.33
AD-13	4.32	1086	10.71	1.25
AD-14	2.41	1946	15.01	1.25

Dynamic Properties. The translational diffusion coefficients at finite polymer concentrations for molecular weights $<8.42 \times 10^6$ were determined by using the cumulant analysis to fit the data in the region $qR_g \ll 1$. For the remaining polymer samples, the $G^2(\tau)$ data were fit by using the multiexponential sampling technique. The infinite dilution translational diffusion coefficient was obtained from

$$\langle D_t \rangle_z = \langle D_t^0 \rangle (1 + k_D c) \quad (20)$$

where K_D can be evaluated by

$$K_d = 1/\langle D_t^0 \rangle_z (\mathrm{d}\langle D_t \rangle_z / \mathrm{d}c)_T \quad (21)$$

and the average hydrodynamic radius $\bar{R}_h$ ($= \langle R_h^{-1} \rangle_z^{-1}$) can be obtained from the Stokes–Einstein[31] equation

$$\langle D_t \rangle_z = kT/6\pi\eta_0 \bar{R}_h \quad (22)$$

where η_0 is the measured solvent viscosity. The experimentally determined values of D_t^0, $\bar{R}_h$, k_D, and M_w are listed in Table II. For both polymer samples, AD-13 and AD-14, a bimodal distribution was obtained at the smallest scattering angle ($\theta = 30°$ and 20°, respectively) and here the $D(c)$ values were computed from the first cumulant of the slow component of $G(\Gamma)$. Figure 4 shows a plot of D_t versus concentration for samples AD-11, AD-12, AD-13,

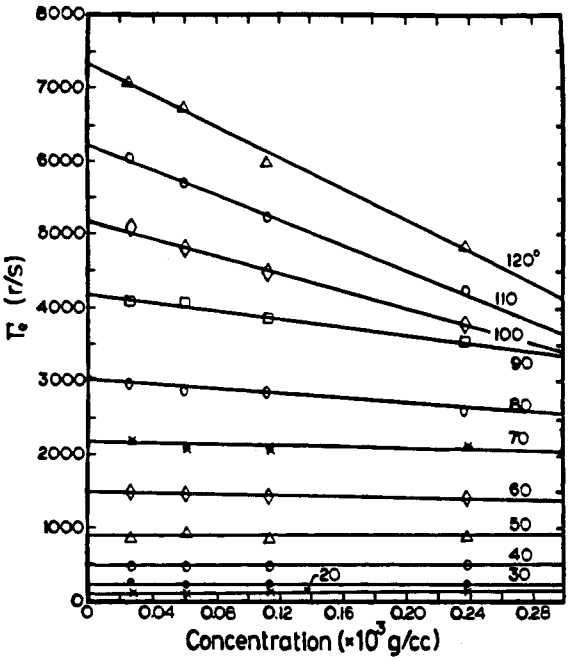

Figure 5. Γ_e extrapolated to infinite dilution for sample AD-14 at 11 scattering angles from 20° to 120°.

and AD-14. Figure 5 shows the concentration dependence of $\Gamma_e(q,c)$ at constant q for the highest molecular weight sample AD-14. The data at each angle are well represented by equations linear in c. The slopes change sign from positive to negative with increasing qR_g. Similar observations have also been made for PS in benzene[36] and polyisoprenes in cyclohexane[37] in the intermediate qR_g region. We have determined $\Gamma_{e,c\to 0}$ and compared values obtained from cumulant fits (up to fourth-order terms) with double-exponential and multiexponential fits. As expected, the second-order cumulant fit consistently underestimates the characteristic decay rate. The best fits to the experimental data were obtained by using the multiexponential sampling technique and the results from this analysis were compared with current theoretical predictions for the behavior of Γ^* in the region $qR_g \gg 1$.

Discussion

The static and dynamic light scattering parameters, R_g, A_2, D_t^0, and R_h, have been evaluated by utilizing scrupulously dry (THF) solvent. It is of interest to compare values of the universal ratios for PS in dry THF with earlier results. We find that these ratios are comparable to those determined earlier and are therefore still in serious disagreement with the RG theory predictions[6] for self-avoiding coils in the nondraining limit. For example, the universal ratios Ψ and U_{fs} defined by

$$\Psi = A_2M^2/4\pi^{3/2}N_A\langle R_g^2\rangle^{3/2} \tag{23}$$

$$U_{fs} = 6\pi R_h/\langle R_g^2\rangle^{1/2} \tag{24}$$

are predicted[6] to be $\Psi = 0.219$ and $U_{fs} = 12.067$. In comparison, light scattering results for PS in THF indicate $\Psi = 0.315 \pm 0.027$ and $U_{fs} = 14.71 \pm 0.048$.

To understand the implications of these observations it is useful to briefly review results of earlier studies in the literature. Experiments on a variety of systems at the Θ condition appear to show consistently[41,42] that the ratio of the static to dynamic radii is $\rho = R_g/R_h \cong 1.27$, corresponding to $U_{fs} = 14.84$. This value agrees with Monte Carlo calculations by Zimm[24] for nondraining Gaussian coils, based on a nonpreaveraged Oseen tensor without hydrodynamic screening. In many good-solvent systems[12-17] the experimentally observed ratio, ρ, is found to have values of $\cong 1.5$, corresponding to $U_{fs} = 12.57$. This value is in agreement with RG calculations[6] for nondraining self-avoiding chains with a nonpreaveraged Oseen tensor and no hydrodynamic screening. Theory predicts[6] a monotonic increase of ρ from 1.27 to 1.5 with increasing solvent quality. It might appear therefore, that a satisfactory understanding of coil hydrodynamics has been achieved. However, several experimental and theoretical studies are in conflict with this viewpoint. In particular, the experimental data of Noda et al.[43-45] for poly(α-methylstyrene) solutions result in $\rho \cong 1.5$ for both Θ- and good-solvent systems. Our light scattering experiments for PS in the good solvent, THF, exhibit $\rho = R_g/R_h \cong 1.3$ while similar experiments utilizing the same polymer samples in ethylbenzene,[17] another good solvent, show $\rho = 1.57$. From the theoretical viewpoint,[73,74] it has been pointed out that Zimm's prediction represents a lower bound to the exact result for Gaussian nondraining chains. Brownian dynamical simulations with nonpreaveraged Oseen hydrodynamic interactions do not yet reproduce the Zimm result.[74] To achieve ρ values consistent with the experimental value $\rho \cong 1.3$ in θ solvents, Fixman[65] had to incorporate internal friction into the hydrodynamics. With regard to the good-solvent limit, it is noted that RG calculations are generally evaluated as a perturbation series and, as in the analysis of Oono et al.[6] are often truncated at the first order. Also, a recent RG calculation by Douglas and Freed[7] concludes that the ratio $\rho = R_g/\bar{R}_h$ is in fact independent of changes in the strength of the excluded-volume interaction and can vary only if hydrodynamic draining effects are present. This latter point of view is similar to that deduced from evaluation[37] of the classical Kirkwood result for long nondraining chains using the preaveraged Oseen tensor

$$R_h^{-1} = N^{-2}\sum_{i<j}\langle 1/R_{ij}\rangle \tag{25}$$

when the Gaussian distribution is used for chains in Θ solvents, and the Domb–Gillis–Wilmers[66] distribution is used for chains in good solvents. Again ρ is determined to be essentially identical in good and Θ solvents in the nondraining limit. Thus, our determination of $\rho = 1.3$ for the PS–THF system and $\rho = 1.57$ for PS in ethylbenzene indicates that the details of the internal hydrodynamic interactions of chain molecules in good solvents may be nonuniversal.

Turning to our dynamic light scattering data at large scattering vectors, we have reported for the first time information on the behavior of Γ^* for the PS–THF system in the intermediate qR_g region where $\Gamma_e \propto q^3$. Experimental values of Γ_e for PS in THF at $qR_g \gtrsim 1.0$ indeed show q^3 dependence as well as significant variation with polymer concentration. Extrapolation to $c = 0$ yields values of $\Gamma_e(q,c=0)$ and Figure 6 shows the q dependence of the normalized values $\Gamma^{**}=\Gamma_e(q,c=0)/q^2D_t^0$. In the region $qR_g \ll 1$ these values are independent of q and increase linearly with q in the intermediate qR_g region. This behavior is consistent with the scaling law[5a] deduced for long flexible nondraining chains

$$\Gamma \propto q^{2+\nu_h/\nu_g} \tag{26}$$

where ν_h and ν_g represent the exponents in the molecular weight dependence of the hydrodynamic radius, R_h, and the radius of gyration, R_g, respectively. For the PS–THF system we obtained $\nu_g = 0.57$ and $\nu_h = 0.56$. The precise slope of the plot at $qR_g > 1$ in Figure 6 is very close to 2.9, in good agreement with eq 26, which has also been con-

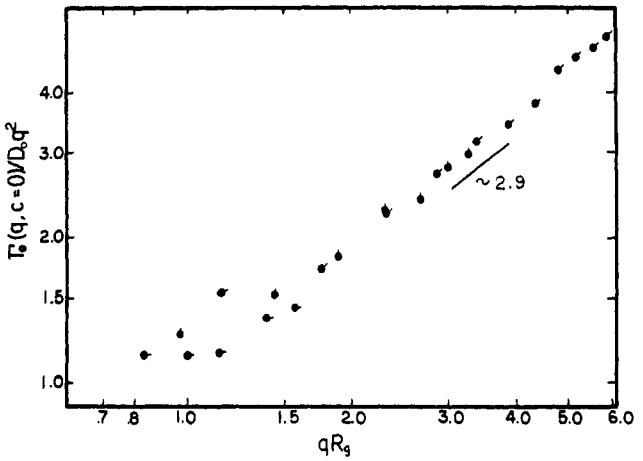

Figure 6. Plot of the normalized value $\Gamma_{e,c=0}/q^2D_t^0$ against qR_g for samples AD-12, AD-13, and AD-14. Solid line has slope = 2.9.

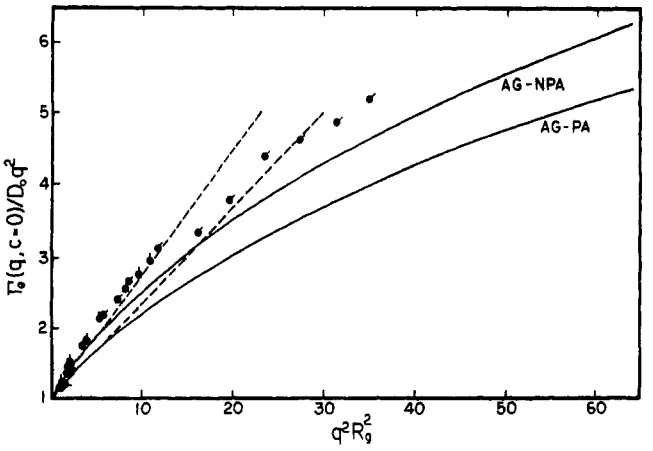

Figure 7. Plot of the reduced values $\Gamma_{e,c=0}/q^2D_t^0$ against $q^2R_g^2$. Shown are the data for samples AD-12 (•), AD-13 (▲), and AD-14 (▼). The solid lines AG–PA and AG–NPA are the theoretical curves of Akcasu and Gurol (AG)[56] for nondraining Gaussian chains with preaveraged (PA) and non-PA Oseen hydrodynamic interactions, respectively. The broken lines represent the initial slopes, $C = 2/15$ and $C = 13/75$, for the AG–PA and AG–NPA curves, respectively.

firmed by experiments[13,46,52,75] done on other solvent systems. However, as noted below, deviations between the values of Γ^{**} determined for our system and those obtained elsewhere suggest that the theoretical arguments leading to eq 26 may be incomplete.

To see this, we first show in Figure 7 the variation of $\Gamma_e(q,0)/q^2D_t^0$ with $q^2R_g^2$ in the range $(qR_g)^2 < 40.0$ for the samples AD-12, AD-13, and AD-14. For $qR_g \ll 1$ the $\Gamma_e(q,0)$ value becomes equivalent to $D_t^0q^2$. The increase of $\Gamma_e(q,0)/q^2D_t^0$ with q due to internal motions was analyzed at small $q^2R_g^2$ by

$$\Gamma_e(q,0)/q^2D_t^0 = (1 + C(qR_g)^2 + ...) \qquad (27)$$

from which the dimensionless parameter C was estimated.[55] Clearly, our data are located closer to the theoretical curve (AG–NPA) for nondraining Gaussian chains with the nonpreaveraged Oseen tensor whose initial slope $C = 0.173$. A similar conclusion was reached in the study of Tsunashima et al.[37] for polyisoprenes (PIP) in the good solvent cyclohexane (CH). However, at values of $q^2R_g^2 \gtrsim 5$ our Γ^{**} data systematically deviate from predictions of the AG–NPA theory. This behavior is distinctly different from that observed for PIP in CH where Γ^{**} values at $q^2R_g^2 < 60$ are always close to the AG–NPA curve. It is further pertinent to note that the Γ^{**} data of Nemoto et al.[36] for

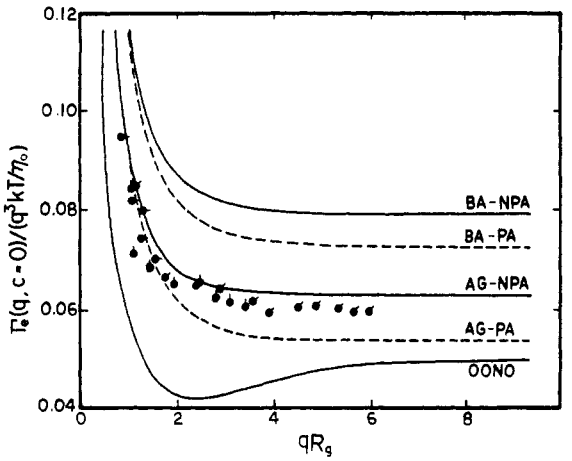

Figure 8. Reduced decay rate $\Gamma_e(q,0)/q^3kT/\eta_0$ as a function of qR_g. Symbols are the same as in Figure 7. The solid lines AG–NPA[56] and BA–NPA[59,62] represent the theoretical curves for nondraining chains in the Θ- and good-solvent limits, using nonpreaveraged Oseen hydrodynamics. AG–PA and BA–PA correspond to similar calculations using a preaveraged Oseen tensor. The solid line OONO[63] is for self-avoiding chains with the non-PA Oseen tensor.

polystyrene in benzene lie very close to the AG–PA curve in Figure 7, whose initial slope is $C = 0.133$. Theoretically, although Tanaka and Stockmayer[58] predict that the quantity C depends to a negligible extent on the excluded-volume effect, a definitive value of C for chains in good solvents does not appear to have been established to date.

Evidently, for three polymer–solvent systems, (PS–THF, PS–BZ, PIP–CH) which each lie close to the asymptotic good-solvent limit ($R_g \simeq M^{0.588}$, $A_2 \simeq M^{-0.221}$), Γ^{**} versus $q^2R_g^2$ data suggest differences in the nature of chain hydrodynamics. Two experimental effects can contribute to the nonuniversality observed in Figure 7. One source derives from variations in the ratio $\rho = R_g/R_h$. Our results for PS–THF indicate ρ values 13–15% lower than those predicted by the AG–NPA theory. However, the value of ρ determined for PIP in CH[37] is ≅1.5, and for PS in BZ[36] $\rho \cong 1.55$. A second contribution can arise from variations in the effective decay rate Γ_e, corrected for solvent viscosity and concentration. This effect can be seen in plots of the reduced first cumulant $\Gamma^* = \Gamma_e(q,c=0)/q^3kT/\eta_0$ versus qR_g as shown in Figure 8. For PS in THF these values for samples AD-12, AD-13, and AD-14 superpose on a master curve which decreases rapidly for $qR_g < 2$ and approaches an asymptote at $qR_g \cong 4$. The solid lines shown on this figure are the theoretical curves obtained for nondraining Gaussian chains with non-PA Oseen hydrodynamics in the Θ- (AG)[56] and good- (BA)[59,62] solvent limits. Also shown is a curve obtained by Oono et al.[63,73] for a nondraining self-avoiding chain with a NPA Oseen tensor using the RG approach. The predicted asymptotic values are 0.0625 for AG–NPA, 0.079 for the BA–NPA, and 0.05 for the Oono curve, respectively. The broken lines on the same figure are the AG and BA curves with a preaveraged (PA) Oseen tensor whose asymptotes are 0.053 and 0.071, respectively. Our experimental data for PS in THF are quite close to the AG–NPA prediction for Gaussian chains with nonpreaveraged Oseen hydrodynamic interactions and very far from the BA–NPA or the Oono predictions for self-avoiding chains. For comparison, Γ^* values deduced by Tsunashima et al.[37] for highly swollen polyisoprene chains appear very similar to our results and reach an asymptote which we estimate to be 0.061. On the other hand, Nemoto's Γ^* data for PS in benzene[36] lie below the theoretical estimates of AG–NPA and are in fact very close to the

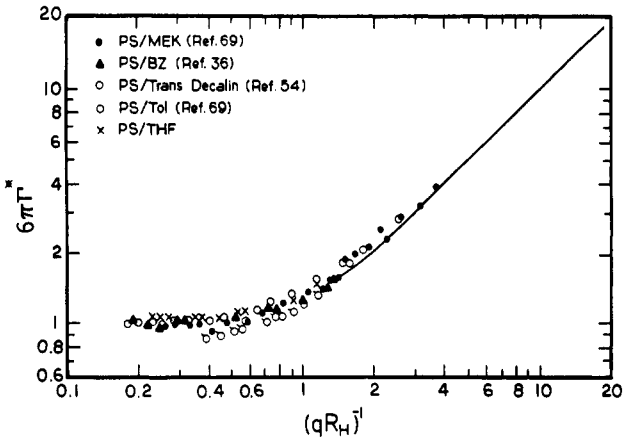

Figure 9. Plot of the dimensionless parameter $6\pi\eta_0\Gamma_e(q,0)/q^3kT$ versus $1/qR_h$ for PS-benzene, PS-methyl ethyl ketone, PS-toluene, PS-*trans*-decalin, and PS-tetrahydrofuran. The solid line is a guide to the eye that the data superpose to form a master curve.

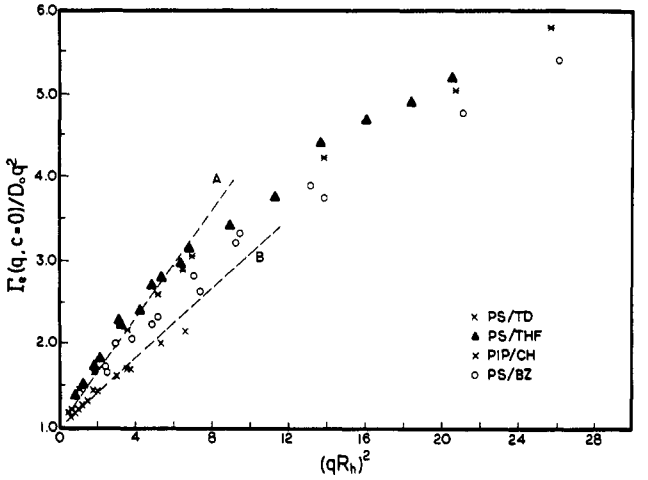

Figure 10. Reduced values of Γ^{**} plotted against $q^2R_h^2$ in the range $q^2R_h^2 < 30$. Shown are the data for (○) PS-BZ, (▲) PS-THF, (*) PIP-CH, and (×) PS-TD. The broken lines A and B represent the initial slopes of the data in the good and Θ solvents, respectively.

AG-PA[56] curve. We estimate that the Γ^* values for PS in BZ reach an asymptote at $\simeq 0.055$.

In discussing Figure 8, we first note that experimental uncertainties in the determination of Γ^* are quite small ($\simeq$2-4%) when Γ_e is computed via fits to a multiexponential distribution. Hence it is reasonable to attribute significance to differences in Γ^* of the order of 15% (e.g. 0.055 versus 0.06). It follows, therefore, that Figures 7 and 8 indicate a variety of nonuniversal hydrodynamic behaviors for these polymer-solvent systems. PS in THF and PIP in CH have the largest asymptotic values of Γ^* but differ substantially in ρ; PS-BZ has a ρ value similar to PIP-CH, but a smaller Γ^* asymptote; Θ-solvent systems for both PS and PIP have comparable ρ values ($\rho \simeq 1.3$) and comparable small values of the Γ^* asymptote ($\simeq 0.045$). Second, we remind the reader that the agreement between experimental data for the good-solvent systems, PS-THF and PIP-CH with the AG-NPA, which assumes a Gaussian chain, must be regarded as fortuitous. In fact, experimental data corresponding to Figure 8 for PS and PIP in Θ solvents falls substantially below the AG-NPA prediction and are closer to the AG-PA curves. A rationale for the apparent applicability of the AG-NPA theory to polymers in good solvents has been suggested[37] before. This is based on the argument that there is a negligible effect of excluded volume on the value of ρ for flexible chains,[7,8] so that variations in ρ must be interpreted as due to differences in the nature of the segmental hydrodynamic interaction, e.g., different amounts of internal friction[65] or draining.[72] If internal friction is absent in expanded coils, then a nondraining Gaussian model might be appropriate. This is not consistent with our results for PS in THF where we determine $\rho \simeq 1.3$ and $\Gamma^* \simeq 0.059$. Other effects need to be considered. For example, literature data for PS in BZ fall on the AG-PA curve in Figure 7 and it has been suggested that the rigidity of the PS chain may be a factor. Our results for PS in THF indicate that additional phenomena, such as solvent draining and hydrodynamic screening, may also need to be included.

Finally, in Figure 9, as proposed by Wiltzius and Cannell,[69] we have compared our experimental values of the quantity Γ^* versus $1/qR_h$ with literature data on various polymer-solvent systems. Results for the good-solvent systems, PS-benzene[36] and PS-toluene,[69] have been plotted along with data for the marginal-solvent system PS-MEK[69] and the Θ-solvent system PS-*trans*-decalin.[54] The values of ρ used to determine the equivalent qR_h values were obtained from the references noted above. From Figure 9, apparently all these results superpose to produce a universal master curve. There are at least three reasons that selection of qR_h values rather than qR_g as the reduced variable aids the superposition. First, as noted by Wiltzius et al.[69] the hydrodynamic radius does not reach its asymptotic molecular weight dependence nearly as fast as the radius of gyration.[69,36] Thus, variations in the excluded-volume interaction for different systems are minimized in this plot. Second, the parameter qR_h may compensate for differences in the strength of the hydrodynamic interaction between different polymer-solvent systems. Third, R_h is measured as the inverse z-average and is less sensitive to variations in the polydispersity of the polymer samples. However, log-log plots of the type shown in Figure 9 cannot resolve differences of the order of 15% noted earlier in the Γ^* asymptotes.

On the basis of these results, we anticipate that a similar scaling of the static length scale in Figure 7 should lead to a more systematic treatment of the quantity $\Gamma^{**} = \Gamma_e(q,c=0)/q^2D_t^0$. This hypothesis is tested in Figure 10 where a plot of Γ^{**} versus $(qR_h)^2$ is shown for our data as well as for Γ^{**} data for various other polymer-solvent systems from references noted in the previous paragraph. The scaled scattering vector, qR_h, appears to provide a more useful index of the crossover in the internal dynamics to the intermediate q nondraining asymptote. Thus Figure 10 indicates that the Γ^{**} data for these systems can be represented as a series of curves whose behavior appears to be determined by the effect of excluded volume on the Γ^* asymptote. If these data are analyzed at small $q^2R_h^2$ by

$$\Gamma_e(q,c=0)/q^2D_t^0 = (1 + C^*(qR_h)^2 + ...) \qquad (28)$$

the initial slope C^* can be estimated. For the most strongly swollen systems (PS-THF and PIP-CH) we estimate the initial slope, C^*, to be almost twice that for the Θ solvents[54] where $C^* \cong 0.174$. The Γ^* data for PS-benzene suggest that this system represents a slightly poorer solvent than PS-THF, consistent with comparative estimates of the interpenetration parameter, Ψ, as described above. Experimental results for Γ^{**} at $(qR_h)^2 > 10$ appear to be consistent with experimental[36,54,69] and theoretical estimates[56,59,62] of the effect of the excluded volume on the asymptotic value of Γ^*.

In conclusion, we find that the dynamic light scattering properties of dilute PS solutions in THF extending from

the small to the intermediate qR_g region cannot be described by the existing hydrodynamic theory. Our experimental values of the reduced decay rate Γ^* are similar to values predicted by a nondraining Gaussian chain model with a nonpreaveraged Oseen hydrodynamic interaction, but data on the ratio $\rho = R_g/R_h$ are not consistent with this theory. On the other hand, our results for ρ are consistent with predictions for nondraining self-avoiding chains[7,8] but our Γ^* data do not agree with a calculation[63] for swollen chains. The nature of the discrepancies between experimental and theoretical values of ρ and Γ^* described here for PS–THF are distinctly different from those described in recent literature for good- and Θ-solvent systems. To rationalize these disparate observations, current hydrodynamic theory will need to be modified to include phenomena such as internal friction, chain rigidity, variations in the degree of draining, and hydrodynamic screening.

Acknowledgment. We thank the National Science Foundation for support of this work through research award NSF DMR 86-14093.

Registry No. PS, 9003-53-6.

References and Notes

(1) Yamakawa, H. *Modern Theory of Polymer Solutions*; Harper and Row: New York, 1971.
(2) Guttmann, C. M.; McCrackin, F. L.; Han, C. C. *Macromolecules* **1982**, *15*, 1205.
(3) Barrett, A. J. *Macromolecules* **1984**, *17*, 1566.
(4) Barrett, A. J. *Macromolecules* **1984**, *17*, 1551.
(5) (a) de Gennes, P.-G. *Phys. Lett. A* **1972**, *38A*, 339; (b) *Scaling Concepts in Polymer Physics*; Cornell University: Ithaca, NY, 1979.
(6) Oono, Y.; Kohmoto, M. *J. Chem. Phys.* **1983**, *78*, 520.
(7) Douglas, J. F.; Freed, K. F. *Macromolecules* **1984**, *17*, 2344.
(8) Douglas, J. F.; Freed, K. F. *Macromolecules* **1984**, *17*, 2354.
(9) Kirkwood, J. G.; Riseman, J. *J. Chem. Phys* **1948**, *16*, 565.
(10) Barrett, A. J.; Domb, C. *Proc. R. Soc. London A* **1981**, *376*, 366.
(11) Lax, M.; Barrett, A. J.; Domb, C. *J. Phys. A: Math. Gen.* **1978**, *11*, 361.
(12) Miyaki, Y.; Einage, Y.; Fujita, H. *Macromolecules* **1978**, *11*, 1180.
(13) Adam, M.; Delsanti, M. *Macromolecules* **1977**, *10*, 1229.
(14) Fukuda, M.; Fukutomi, F.; Kato, Y.; Hashimoto, M. *J. Polym. Sci., Polym. Phys. Ed.* **1974**, *12*, 871.
(15) Appelt, B.; Meyerhoff, G. *Macromolecules* **1980**, *13*, 657.
(16) Utiyama, H.; Utsumi, H.; Tsunashima, Y.; Kurata, M. *Macromolecules* **1978**, *11*, 506.
(17) Venkataswamy, K.; Jamieson, A. M. *Macromolecules* **1986**, *19*, 124.
(18) Mandema, W.; Zeldenrust, H. *Polymer* **1977**, *18*, 835.
(19) Koppel, D. E. *J. Chem. Phys.* **1972**, *57*, 4814.
(20) McDonnell, M. E.; Ramanatham, M. *Macromolecules* **1984**, *17*, 2093.
(21) McDonnell, M. E.; Jamieson, A. M. *J. Macromol. Sci., Phys.* **1977**, *B13*, 67.
(22) Yu, T. L.; Reihanian, H.; Jamieson, A. M. *Macromolecules* **1980**, *13*, 1590.
(23) Jamieson, A. M.; Venkataswamy, K. *Polym. Bull. (Berlin)* **1984**, *12*, 275.
(24) Zimm, B. H. *Macromolecules* **1980**, *13*, 592.
(25) Spychaj, T.; Lath, D.; Berek, D. *Polymer* **1979**, *20*, 437.
(26) Zimm, B. H. *J. Chem. Phys.* **1948**, *16*, 1099.
(27) Berry, G. C. *J. Chem. Phys.* **1966**, *44*, 12, 4550.
(28) Meyerhoff, G.; Appelt, B. *Macromolecules* **1979**, *12*, 1968.
(29) Schulz, G. B.; Baumann, H. *Makromol. Chem.* **1968**, *114*, 122.
(30) Stacey, C. J.; Kraus, G. *J. Polym. Sci., Polym. Phys. Ed.* **1979**, *17*, 2007.
(31) Tanford, C. *Physical Chemistry of Macromolecules*; Wiley: New York, 1961.
(32) Pike, E. R.; Pomeroy, W. R.; Vaughan, J. M. *J. Chem. Phys.* **1975**, *62*, 3188.
(33) Ostrowsky, N.; Sornette, D.; Parker, P.; Pike, E. R. *Opt. Acta* **1981**, *28*, 1059.
(34) McWhirter, J. G.; Pike, E. R. *J. Phys. A: Math Gen.* **1978**, *11*, 1729. (a) Dahneke, B. E. *Measurement of Suspended Particles by QELS*; Wiley: New York, 1983; pp 107–127.
(35) McWhirter, J. G. *Opt. Acta* **1980**, *27*, 83.
(36) Nemoto, N.; Makita, Y.; Tsunashima, Y.; Kurata, M. *Macromolecules* **1984**, *17*, 425.
(37) Tsunashima, Y.; Hirata, M.; Nemoto, N.; Kurata, M. *Macromolecules* **1987**, *20*, 1992.
(38) Matsumoto, T.; Nishioka, M.; Fujita, H. *J. Polym. Sci., Part B* **1972**, *10*, 23.
(39) Miyaki, Y., Einaga, T.; Hiroseye, T.; Fujita, H. *Macromolecules* **1977**, *10*, 1356.
(40) Ter Meer, H. U.; Burchard, W.; Wunderlich, W. *Colloid Polym. Sci.* **1980**, *258*, 675.
(41) Schmidt, M.; Burchard, W. *Macromolecules* **1981**, *14*, 210.
(42) Han, C. C. *Polymer* **1979**, *20*, 259.
(43) Kato, T.; Miyaso, K.; Noda, I.; Fujimoto, T.; Nagasawa, M. *Macromolecules* **1970**, *3*, 777.
(44) Noda, I.; Fujimoto, T.; Nagasawa, M. *Macromolecules* **1970**, *3*(6), 787.
(45) Noda, I.; Mizutani, K.; Kato, T. *Macromolecules* **1977**, *10*(3), 618.
(46) Han, C. C.; Akcasu, A. Z. *Macromolecules* **1981**, *14*, 1080.
(47) Buldt, G. *Macromolecules* **1976**, *9*, 606.
(48) Hendrix, J.; Saleh, B. *Polymer* **1977**, *18*, 10.
(49) Freire, J. J. *Polymer* **1978**, *19*, 1441.
(50) Gulari, E.; Gulari, E.; Tsunashima, Y.; Chu, B. *J. Chem. Phys.* **1979**, *70*, 3965.
(51) Gulari, E.; Gulari, E.; Tsunashima, Y.; Chu, B. *Polymer* **1979**, *20*, 347.
(52) Nose, T.; Chu, B. *Macromolecules* **1979**, *12*, 1122.
(53) Tsunashima, Y.; Hirata, M.; Nemoto, N.; Kurata, M. *Macromolecules* **1983**, *16*, 584.
(54) Tsunashima, Y.; Nemoto, N.; Kurata, M. *Macromolecules* **1983**, *16*, 1184.
(55) Burchard, W.; Schmidt, M.; Stockmayer, W. H. *Macromolecules* **1980**, *13*, 580.
(56) Akcasu, A. Z.; Gurol, H. *J. Polym. Sci., Polym. Phys. Ed.* **1976**, *14*, 1.
(57) Bantle, S.; Schmidt, M.; Burchard, W. *Macromolecules* **1982**, *15*, 1604.
(58) Tanaka, G.; Stockmayer, W. H. *Proc. Natl. Acad. Sci. U.S.A.* **1982**, *79*, 6401.
(59) Benmouna, M.; Akcasu, A. Z. *Macromolecules* **1980**, *13*, 409.
(60) Akcasu, A. Z.; Han, C. C.; Benmouna, M. *Polymer* **1980**, *21*, 866.
(61) Utiyama, H.; Tsuanshima, Y.; Kurata, M. *J. Chem. Phys.* **1971**, *55*, 3133.
(62) Benmouna, M.; Akcasu, A. Z. *Macromolecules* **1978**, *11*, 1187.
(63) Lee, A.; Baldwin, P. R.; Oono, Y. *Phys. Rev. A* **1984**, *30*(2), 968.
(64) Schafer, L. *Macromolecules* **1984**, *17*, 1357.
(65) Fixman, M. *J. Chem. Phys.* **1986**, *84*, 4085.
(66) Domb, C.; Gillis, J.; Wilmers, G. *Proc. Phys. Soc., London* **1965**, *85*, 625.
(67) Dubois-Voilette, E.; DeGennes, P. G. *Physics (Long Island City, N.Y.)* **1967**, *3*, 181.
(68) Miyake, A.; Freed, K. F. *Macromolecules* **1983**, *16*, 1228.
(69) Wiltzius, P.; Cannell, D. S. *Phys. Rev. Lett.* **1986**, *56*(1), 61.
(70) Chu, B.; Wu, D. Q. *Macromolecules* **1987**, *20*, 1606.
(71) Provencher, S. W. *J. Chem. Phys.* **1976**, *64*, 2772.
(72) Freed, K. F.; Douglas, J. F.; Wang, S. Q.; Perico, A. *Polymer-Flow Interaction*; AIP Conference Proceedings No. 137; American Institute of Physics: New York, 1985.
(73) Tsunashima, Y.; Hirata, M.; Nemoto, N.; Kanjiwara, K.; Kurata, M. *Macromolecules* **1987**, *20*, 2862.
(74) Oono, Y. *Adv. Chem. Ser.* **1987**, *1*.
(75) Numasawa, N.; Hamada, T., Nose, T. *J. Polym. Sci., Polym. Phys. Ed.* **1986**, *24*, 19.